SCPL: Indoor Device-Free Multi-Subject Counting and Localization Using Radio Signal Strength

Chenren Xu†, Bernhard Firner†, Robert S. Moore∗, Yanyong Zhang†

Wade Trappe†, Richard Howard†, Feixiong Zhang†, Ning An§

†WINLAB, Rutgers University, North Brunswick, NJ, USA
∗Computer Science Dept, Rutgers University, Piscataway, NJ, USA
§Gerontechnology Lab, Hefei University of Technology, Hefei, Anhui, China

ABSTRACT

Radio frequency based device-free passive (DfP) localization techniques have shown great potentials in localizing individual human subjects, without requiring them to carry any radio devices. In this study, we extend the DfP technique to count and localize multiple subjects in indoor environments. To address the impact of multipath on indoor radio signals, we adopt a fingerprinting based approach to infer subject locations from observed signal strengths through profiling the environment. When multiple subjects are present, our objective is to use the profiling data collected by *a single* subject to count and localize *multiple* subjects without any extra effort. In order to address the non-linearity of the impact of multiple subjects, we propose a successive cancellation based algorithm to iteratively determine the number of subjects. We model indoor human trajectories as a state transition process, exploit indoor human mobility constraints and integrate all information into a conditional random field (CRF) to simultaneously localize multiple subjects. As a result, we call the proposed algorithm *SCPL* – sequential counting, parallel localizing.

We test SCPL with two different indoor settings, one with size 150 m^2 and the other 400 m^2. In each setting, we have four different subjects, walking around in the deployed areas, sometimes with overlapping trajectories. Through extensive experimental results, we show that SCPL can count the present subjects with 86% counting percentage when their trajectories are not completely overlapping. Our localization algorithms are also highly accurate, with an average localization error distance of 1.3 m.

Categories and Subject Descriptors

C.3 [**Special-Purpose and Application-Based Systems**]: Realtime and embedded systems

General Terms

Algorithm, Experimentation, Measurement

Keywords

Device-free Localization, Counting, Tracking, Trajectory, Multiple Subjects, Fingerprint, Nonlinear Fading

1. INTRODUCTION

Ambient Intelligence (AmI) envisions that future smart environments will be sensitive and responsive to the presence of people, thereby enhancing everyday life. Potential applications include eldercare, rescue operations, security enforcement, building occupancy statistics, etc. The key to enable these ubiquitous applications is the ability to localize various subjects and objects in the environment of interest. Device-free passive (DfP) localization has been proposed as a way of detecting and tracking subjects without the need to carry any tags or devices. It has the additional advantage of being unobtrusive while offering good privacy protection. Over the past decades, researchers have studied ways of tracking device-free human subjects using different techniques such as camera [9], capacitance [21], pressure [15], infrared [3] and ultrasonic [6]. However, they all suffer from serious limitations such as occlusion [9, 3], high deployment cost [15, 21] or short range [6].

Radio frequency (RF)-based techniques have the advantages of long-range, low-cost, and the ability to work through non-conducting walls and obstacles Several RF-based DfP localization techniques have been proposed in [29, 31, 16, 11, 23, 2, 24, 27, 7], and these approaches observe how people disturb the pattern of radio waves in an indoor space and derive their positions accordingly. To do so, they collect training data to profile the deployed area, and form mathematical models to relate observed signal strength values to locations. DfP algorithms can be broadly categorized into two groups: *location-based*, and *link-based*. Location-based DfP schemes collect a radio map with the subject present in various predetermined locations, and then map the test location to one of these trained locations based upon observed radio signals, which is also known as fingerprinting, as studied in [29, 27]. Link-based DfP schemes, however, capture the statistical relationship between the received signal strength (RSS) of a radio link and whether the subject is on the Line-of-Sight (LoS) of the radio link, and consequently determine the subject's location using geometric approaches [31, 16, 2, 7].

Recognizing that merely tracking an individual might not be sufficient for typical indoor scenarios, researchers have been pushing a great amount of effort towards scaling to multiple device-free subjects, such as in [32, 30, 13, 24, 27, 14]. They observe the change of RSS mean or variance and propose different tracking algorithms.

The common thing missing is that the number of subjects is known, which is a strong assumption. In addition, in cluttered indoor environments, subjects can cause collective nonlinear fading effects, which might significantly degrade the tracking performance and is not explicitly treated in the work above. On the other hand, location-based schemes can be straightforward but prohibitive due to the exponential increase in the training overhead if we need to profile the system with different combinations of these subjects.

In this study, we propose and evaluate an efficient DfP scheme for tracking multiple subjects using the training data collected by a single subject to avoid expensive training overhead.

Our algorithm consists of two phases. In the first phase, we *count* how many subjects are present using successive cancellation in an iterative fashion. In each iteration, we detect whether the room is empty. If it is not empty, we identify the location for one subject, and then subtract her impact on the RSS values from the collective impact measured in the experiment. Care must be taken when subtracting a subject's impact as the change in the RSS values caused by multiple subjects at the same time is smaller than the sum of RSS changes from each individual subject. In order to compensate for this, we need to multiply a coefficient to a subject's impact and then perform subtraction. The coefficient is specific to the subject's location as well as the link under consideration.

In the second phase, we localize the subjects after their number is known. We partition the deployment area into cells and represent a subject's location using its cell number. We formulate the localization problem as a conditional random field (CRF) by modeling indoor human trajectories as a state transition process and considering mobility constraints such as walls. We then identify the cells occupied by these subjects simultaneously. Since our counting process is sequential and our localization process is parallel, we call our algorithm *SCPL*.

We have tested SCPL in two indoor settings. The first setting is an office environment consisting of cubicles and narrow aisles, which is partitioned into 37 cells. We used the 13 transmitters and 9 receivers that were deployed for some earlier projects. The second setting is an open floor indoor environment, which is partitioned into 56 cells and deployed with 12 transmitters and 8 receivers. In the training phase, we measured the RSS values using a single subject. In the testing phase, we had four subjects with different heights, weights and gender, and designed four different real life office scenarios. These scenarios all had periods of time when multiple subjects walked side by side and thus had overlapping trajectories. We can count the number of subjects accurately, with a 88% counting percentage when the subjects were not walking side by side, and a 80% counting percentage when they were.

Our localization results have good accuracies, with a average error distance of 1.3 m considering all the scenarios. We find that it is beneficial to consider indoor human movement constraints according to the floor map when localizing moving subjects and demonstrate 24% improvement on average compared with no floor map information provided.

Our technique, SCPL, is unique in at least four contributions: (i) to our knowledge, it is the first work to systematically perform simultaneous counting and localization for up to four device-free subjects (moving or stationary) in large-scale deployments only using RF-based techniques; (ii) we designed a set of algorithms to count and localize multiple subjects relying on the calibration data collected by only a single individual; (iii) We also use plausible trajectory constraints (e.g. not walking through walls) based on floor map information, and integrate this information into the radio calibration data to further improve the tracking accuracies; and (iv) we recognize the nonlinear fading effects caused by multiple sub-

jects in cluttered indoor environments, and design the algorithms to mitigate the resulting error.

The rest of the paper is organized as follows. In Section 2, we discuss the applications that benefit from passive localization as well as our solution framework. Our solution consists of two phases, counting the number of subjects (in Section 3) and localizing the subjects (in Section 4). Then we describe our experimental setup in Section 5 and our detailed results in Section 6. We discuss the limitation and future direction of our work in Section 7 and review the related work in Section 8. Finally, we provide the concluding remarks in Section 9.

2. BACKGROUND

Before presenting our SCPL algorithm, we first discuss potential applications and the formulation of the problem.

2.1 Applications that Can Benefit from Passive Localization

Passive localization can find application in many important domains. Below we give a few examples:

Elderly/Health Care: Elder people may fall down in their houses for various reasons, such as tripping, momentary dizziness or overexertion. Without prompt emergency care, this could lead to life-threatening scenarios. Using trajectory based localization information, DfP can perform fall detection quickly because the monitored subject will remain in an unusual location for a long period of time.

Indoor Traffic Flow Statistics: Understanding patterns of human indoor movement can be valuable in identifying hot spots and corridors that help energy management and commercial site selection. DfP provides a non-intrusive and private solution to capturing indoor locations.

Home Security: DfP based home security is a major improvement over camera-based intrusion detection because it can not only detect the intrusion, but also track the intruders.

2.2 Problem Formulation

To solve the passive multi-subject localization problem, we adopt a cell-based fingerprinting approach, similar to the one discussed in [27].

Before we address the multi-subject problem, let us first look at how we localize a single subject. We first partition the deployed area into K cells. In the training phase, we first measure the ambient RSS values for L links when the room is empty. Then a single subject appears in each cell, walks randomly within that cell and takes N RSS measurements from all L radio links. By subtracting the ambient RSS vector from the collected data, we have a profiling dataset $\mathcal{D}$. $\mathcal{D}$, a $K \times N \times L$ matrix, quantifies how much a single subject impacts the radio RSS values from each cell. Having this profiling dataset $\mathcal{D}$, *we model the subject's presence in cell i as state S_i* and thus $\mathcal{D} = \{\mathcal{D}_{S_1}, \mathcal{D}_{S_2}, ..., \mathcal{D}_{S_K}\}$. In the testing phase, we first measure the ambient RSS values when the room is empty. Then a subject appears in a random location, and measures the RSS values for all L links while making random moves in that particular cell. Then we subtract the ambient RSS vector from this measured data, and form an RSS vector, O, which shows how much this subject impacts the radio links from this unknown cell. Based on $\mathcal{D}$ and O, we can run classification algorithms to classify the cell number of the unknown cell, thus localizing the subject.

Next we discuss how we extend the same framework to formulate the multi-subject localization problem. In the training phase,
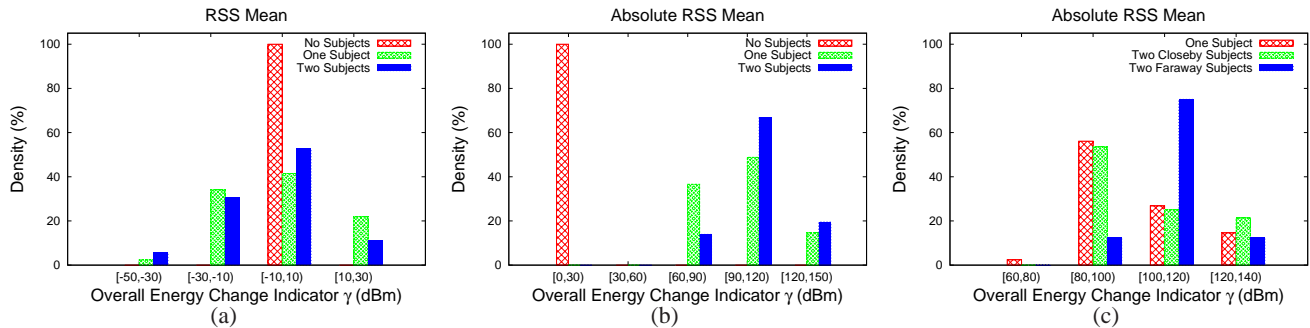
Figure 1: In terms of overall energy change indicator γ, (a) "RSS Mean", for zero, one, and two subjects. (b) "Absolute RSS Mean" for the same measurement shows better discrimination between zero and more than zero subjects. (c) Two subjects separated by more than 4 meters are clearly distinguishable from one subject.

our objective is to still *use a single subject's training data* to keep the training overhead low. Taking the training data for different number of subjects will lead to prohibitive overheads, which we will avoid. In the testing phase, multiple subjects appear in random cells, sometimes in the same cell, and we measure the RSS values for all the radio links. We calculate O in the same way as in the single-subject case.

To calculate the locations for these subjects, we need to go through two phases. In the first phase, we identify the number of subjects that are present simultaneously, C, which we call the *counting* phase. In the second phase, we identify in which cells are these C subjects, which we call the *localizing* phase. Please note that subjects are not stationary, but they move around within the deployed area.

3. COUNTING THE NUMBER OF SUBJECTS

In this section, we first provide empirical data to help the readers understand the impact of having multiple subjects on the radio signals, especially nonlinear fading effect, and then describe our sequential counting algorithm.

3.1 Understanding the Impact of Multiple Subjects on RSS Values

Let us first understand the relationship between a single subject's impact on the room RSS level and multiple subjects' impact. In particular, we would like to find out whether the relationship is linear.

As shown in previous studies such as [29, 31, 22, 2, 27], the RSS level of a radio link changes when a subject is near its Line-of-Sight (LoS). Based on this observation, we make a simple hypothesis: *more subjects will not only affect a larger number of spatially distributed radio links, but they will also lead to a higher level of RSS change on these links.* If this is true, we can infer the number of subjects that are present from the magnitude of the RSS change that we observe in the deployed area. We use the sum of the individual link RSS change to capture the *total energy change* in the environment as

$$\gamma = \sum_{l=1}^{L} O^l,$$

where O^l is the RSS change on link l.

Next we look at how to capture the RSS change of link l. A straightforward metric is to subtract the mean ambient RSS value

for link l (when the room is empty) from the measured mean RSS value for link l, the result of which is referred to as *RSS mean difference*. RSS mean difference is a popular metric that has been used in several studies, e.g., as seen in [29, 22, 2, 27]. However, upon deliberation, we find that RSS mean difference is not suitable for our purpose, mainly because the value is not always positive. Due to the multi-path effect, the presence of a subject does not always weaken a link, but sometimes, it may actually strengthen a link! As a result, the RSS mean difference can be negative. In this case, summing up each link's RSS mean difference does not lead to the correct total energy change in the environment because their values may cancel out each other. To address this issue, we thus propose to use *absolute RSS mean difference* which has a more compact data space than RSS mean when a cell is occupied.

Our experimental results confirm that the absolute RSS mean difference is a more suitable metric. In this set of experiments, we collect the RSS values when there are 0, 1 and 2 subjects who make random movements (with pauses) in the deployed area. We compute the corresponding γ value by using both RSS mean difference and absolute RSS mean difference, and plot their histograms in Figures 1(a)-(b) respectively. In Figure 1(a), when the room is empty, we observe γ values $\in [-10, 10)$ which means the overall energy level is rather stable. However, with 40% to 50% of chances, we still observe $\gamma \in [-10, 10)$ when subjects are present. This is because individual RSS mean differences can cancel out each other, and thus their sum is not a good indicator of the total energy change caused by having multiple subjects.

Absolute RSS mean difference is a better metric, as shown in Figure 1(b). The γ value when there are two subjects is statistically greater than the γ value when there is only one subject. As a result, in the rest of this paper, unless explicitly noted, we use absolute RSS mean difference as the metric to capture the RSS change in the environment. Finally, we note that the γ value alone is inadequate to distinguish between one or two subjects.

By looking at the two-subject data more carefully, we can further separate them into two groups based on the distance between the subjects. If the distance is more than 4 meters (we choose this threshold from the data sets), we call the two subjects *faraway*, and call the subjects *nearby* if the distance is less. We then plot the histograms of these groups in Figure 1(c). When subjects are close to each other, more links will be affected by both subjects, and fewer links are affected by only one of the subjects. Consequently, the γ value in this case will be smaller than the γ value when the two subjects are farther apart. Furthermore, we point out that the

γ value when we have C subjects at the same time is smaller than the sum of the individual γ value from each subject. As a result, it is hard to distinguish having two subjects close to each other from having only one subject.

In summary, we have two main observations from these experiments. First, the absolute RSS mean difference is a suitable metric to capture the impact caused by the appearance of a subject. Second, the total energy change, γ, reflects the level of impact subjects have in the room, but we cannot rely on the value of γ alone to infer how many subjects are present because γ is not linearly proportional to the number of subjects.

3.2 Counting Subjects Using Successive Cancellation

We use successive cancellation to count the number of subjects. When multiple subjects coexist, it often so happens that one subject has a stronger influence on the radio signal than the rest. Thus, our counting algorithm goes through several rounds. In each round, we estimate the strongest subject's cell number in this round assuming there is only a single subject, i, and then subtract her share of RSS change from the remaining RSS vector O to obtain the new remaining RSS vector that will be used in the next round.

If this problem were linear, we could simply subtract the mean vector μ_i associated with cell i in the profiling data $\mathcal{D}$ from the observed RSS vector O. However, as shown in the previous subsection, the total impact from multiple subjects is not linear to the number of subjects – the impact observed when C subjects appear at the same time is smaller than the sum of each subject's impact if they appear one at at time. To be more precise, O is an underestimation of the linear combination of the mean values of the associated cells that we collected in $\mathcal{D}$. To address this issue, instead of subtracting μ_i directly from O, we multiply a coefficient that is less than 1 to μ_i and subtract this normalized term from O. This coefficient, however, is not uniform across all the cell and link combinations; instead, it is specific to each cell and link pair because different cells have different impacts on a link. We will then calculate the location-link coefficient matrix, $\mathcal{B} = (\beta_{i,l})$ where $\beta_{i,l}$ is the coefficient for cell i and link l.

Our algorithm to calculate the coefficient matrix $\mathcal{B}$ is detailed in Algorithm 1. The basic idea is that, for each link l, we compute the correlation between a cell pair, (i, j) with respect to link l. The two cells that both are close to a link are highly correlated with respect to this link. We use h_{ij}^l to denote this correlation[1]. Note that all the RSS values in profiling data are non-negative, and thus we have $h_{ij}^l \geq 0$. For each cell i, we pivot that cell and compute the β_{il} as

$$\beta_{il} = \frac{h_{ii}^l}{\sqrt{\sum_{j=1}^{K} h_{ij}^l{}^2}}.$$

Basically, when two subjects occupy cells i and j respectively, and only one of them affects link l, they have low correlation and the value of h_{ij}^l is close to 0. On the other hand, when they both affect link l, the value of h_{ij}^l will reflect their positive correlation.

Once we determine the location-link coefficient matrix $\mathcal{B}$, we describe our successive cancellation based counting algorithm (shown in Algorithm 2), which can identify the subject count C from the observation RSS vector O using the profiling RSS matrix $\mathcal{D}$ collected by a single subject. We first compute γ^0's and γ^1's from the

---

[1]Notice that we use correlation h_{ij}^l instead of correlation coefficient ρ_{ij}^l because ρ_{ii}^l will always be 1 and thus guarantee its dominance among the all the cells on all the links when the cell i is detected first, which is not true.

Algorithm 1: Location-Link Correlation Algorithm

input : $\mathcal{D}$- The training data collected from L links among K states/cells
output: $\mathcal{B}$ - The location-link coefficient matrix

1 **for** $l = 1 \to L$ **do**
2     $h \leftarrow$ zero matrix of $K \times K$
3   **for** $i = 1 \to K$ **do**
4   **for** $j = 1 \to K$ **do**
5           $I \leftarrow$ training data indices associated with state S_i
6           $J \leftarrow$ training data indices associated with state S_j
7   // Compute the link correlation
8           $h_{ij} \leftarrow E\left[\mathcal{D}_{Il}\mathcal{D}_{Jl}\right]$
9   **for** $i = 1 \to K$ **do**
10        $normfactor \leftarrow \sqrt{\sum_{j=1}^{K} h_{ij}{}^2}$
11   // Compute the location-link coefficient for cell i and link l
12        $\beta_{il} \leftarrow \frac{h_{ii}}{normfactor}$

---

ambient RSS vector and the profiling RSS matrix $\mathcal{D}$ respectively. Then, we construct a 95% confidence interval for the distribution of γ^0's and γ^1's and refer to the associated lower and upper bounds as $c_L^0, c_U^0, c_L^1, c_U^1$. From the observation RSS vector, O, we first compute its γ value and then perform a presence detection: if $\gamma < c_U^0$, we claim the room is empty. Otherwise, we will claim there is at least one subject present and start to iteratively count the number of subjects using successive cancellation to finally determine the value of C.

In each successive cancellation iteration, we do the following:

- *Presence Detection.* We first perform a presence detection by checking if $\gamma \geq c_U^1$ to find out whether there is any more subject in the room. Please note that this condition is stronger than $\gamma \geq c_U^0$, and we will take care of the last iteration separately. If the presence detection returns a 'yes', we increment the detected subject count C, and go to the next step. Otherwise, we end the algorithm.

- *Cell Identification.* If there is a subject in this iteration, we estimate the occupied cell q by

$$q = \operatorname*{argmax}_{i \in \mathcal{S}} P(O|S_i),$$

where $\mathcal{S}$ is the set of remaining unoccupied cells.

- *Contribution Subtraction.* Next, we cancel the impact of this subject from cell q by subtracting $\mu_{ql} \cdot \beta_{ql}$ from O^l for each link l.

In the last round, we simply check if $\gamma < c_U^1$, which actually relax the lower bound of γ^1, which means we consider the possibility that when the last subject is detected in our algorithm, the corresponding γ is lower than the c_L^1. This further compensates for the over-subtraction in our earlier iterations.

4. LOCALIZING MULTIPLE MOVING SUBJECTS WHEN THE SUBJECT COUNT IS KNOWN

In this section, we discuss how we localize multiple moving subjects when the subject count is known. In SCPL, we track multiple subjects in parallel, unlike in the counting phase where we count the number of subjects sequentially. Radio interference is very

Algorithm 2: Successive Cancellation-Based Device-free Passive Counting Algorithm

---

input : $\mathcal{D}$- The training data collected from L links among K cells

$\mathcal{S}$- The states $\{S_1, ..., S_K\}$ associated with the K cells

O- The testing data collected from L links when subjects are in unknown locations

$\mathcal{B}$ - The estimated location-link coefficient matrix generated from Algorithm 1

c_L^0, c_U^0- The lower and upper bounds of the 95% confidence interval when there is no subjects in the deployed area

c_L^1, c_U^1- The lower and upper bounds of the 95% confidence interval when there is one subject in the deployed area

output: C- The estimated number of subjects present in the deployed area

1   $C \leftarrow 0$

2   $\gamma \leftarrow \sum_{l=1}^{L} O^l$

3   // Presence detection

4   **if** $\gamma \leq c_U^0$ **then**

5 | **return** C;

6   // Count the present subjects

7   **else**

8 | **while** *true* **do**

9 | | **if** $\gamma \geq c_U^1$ **then**

10 | | | // Estimate the most likely occupied cell

11 | | | $q \leftarrow \text{argmax}_{i \in \mathcal{S}} \, P(O|S_i)$

12 | | | // Remove the training data associated with the estimated cell in each round

13 | | | $\mathcal{D} \leftarrow \mathcal{D} \backslash \mathcal{D}_q$

14 | | | $\mathcal{S} \leftarrow \mathcal{S} \backslash q$

15 | | | // Update the testing data by removing the partial impact caused by the detected subject in each round

16 | | | **for** $l = 1 \rightarrow L$ **do**

17 | | | | $O^l \leftarrow O^l - \beta_{ql}\mu_{ql}$

18 | | | $C \leftarrow C + 1$

19 | | | // Update the overall affect energy indicator

20 | | | $\gamma \leftarrow \sum_{l=1}^{L} O^l$

21 | | **else if** $\gamma < c_U^1$ **then**

22 | | | $C \leftarrow C + 1$

23 | | | **return** C;

---

complex and unpredictable, especially when multiple subjects are present and a link is affected by multiple people. In this case, it is hard to quantify the exact impact of a subject. Even after considering the cell link coefficient matrix $\mathcal{B}$, we may still overestimate (or, underestimate) a subject's impact on a link. These errors, while insignificant enough not to hurt the counting process, will lead to inferior localization results. On the other hand, parallel tracking keeps all the raw RSS values and can provide better results.

4.1 Understanding the Challenge of Localizing Multiple Subjects

Before presenting our localization algorithm, we first take a closer look at how multiple subjects collectively affect the RSS values and thus complicate the localization problem through empirical data. The complexity of this problem mainly stems from the multi-path effect [17], a typical error source in RF-based indoor localization. In this problem, multi-path can cause nonlinear interference in a radio space when multiple subjects are present. More precisely, when multiple subjects coexist in different locations, the resulting RSS value will not be simply the summation of the individual RSS values from a single subject independently in those locations. The

gap between these two is larger when these subjects are close to each other. To validate this conjecture, we randomly select a few positions with certain distances apart. We first have one subject, A, collect the RSS measurements by standing stationary in these locations. Then, we involve another subject, B with similar height and weight as A, and have them stand in two different positions, say i and j. We use O_i and O_j to denote the measured RSS vector when A is standing in positions i and j independently, and O_{ij} the measured RSS vector when A and B are standing in positions i and j simultaneously. In a linear space, vector O_{ij} would be simply the summation of O_i and O_j. However, as mentioned before, this problem is nonlinear, especially when subjects are close to each other. To quantify the degree of nonlinearity, we define the *RSS Error Residual* as

$$\Delta O^l = O_{ij}^l - O_i^l - O_j^l,$$

for link l. A larger ΔO^l value indicates a higher non-linear degree. To articulate the nonlinearity nature, we remove link l if its O_{ij}^l, O_i^l, O_j^l values are all less than 1 because these links are actually not affected by the subjects in any case. We plot the histograms of the remaining O^l values in Figure 2.

From Figure 2, we have three main observations. Firstly, when the two subjects stand side by side (i.e., the distance between them is 0 m), there are only about 30% and 50% chances that we see $|\Delta O^l| < 2$ for RSS mean and absolute RSS mean respectively, which validates our problem is indeed nonlinear. As the distance becomes longer than 2 m, the probability of having $|\Delta O^l| < 2$ rises to more than 70% for both RSS mean difference and absolute RSS mean difference. Secondly, the error residual can be negative under RSS mean difference, but is positive under absolute RSS mean difference in most cases, suggesting O_{ij} is consistently an underestimation of $O_i + O_j$. This property is desirable because it ensures Monotonicity.

Finally, we define the *total RSS Error Residual* as:

$$\varepsilon = \sum_{l=1}^{L} |\Delta O^l|,$$

which measures the deviation between the profiling data and the RSS measurement in a multi-subject problem. We plot the histogram in Figure 3 and observe that the absolute RSS mean has a smaller ε value, and thus more appropriate for our purposes.

4.2 Conditional Random Field Formulation

Tracking moving subjects actually introduces new optimization opportunities - we can improve our localization results by considering the fact that human locations from adjacent time intervals should form a continuous trajectory, which can be further modeled as a state transition process under conditional random field (CRF) [10]. CRFs are a type of discriminative undirected probabilistic graphical model. We use them to decode the sequential RSS observations into continuous mobility trajectories.

The first step towards formulating a conditional random field is to form the sensor model and transition model respectively. In our problem, we have K states: $\mathcal{S} = \{S_1, S_2, ..., S_K\}$. In a single-subject problem, state S_i means the subject is located in cell i. The sensor model essentially infers the current state based on the observation RSS vector O, which is to generate a cell likelihood map based upon O. For a single subject case, we would like to maximize the likelihood $P(q = S_i|O, \mathcal{D})$ when cell i is occupied. In other words, when the subject is located in cell i in the testing phase, we would like to maximize the probability that the estimated state/cell q matches the actually occupied cell i. We assume the
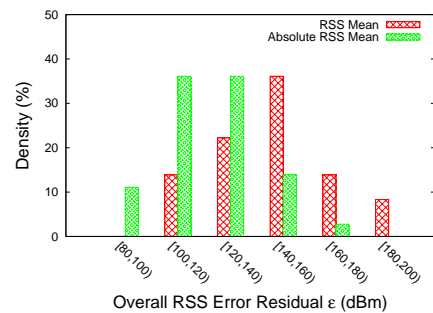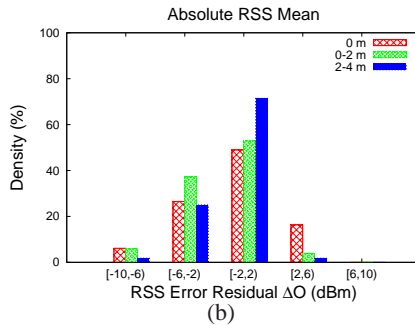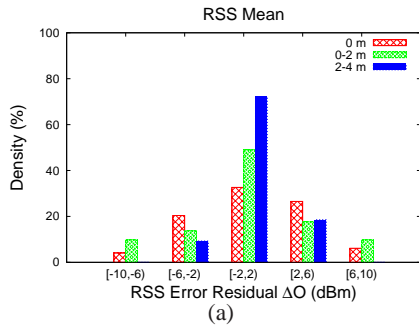
Figure 2: The RSS residual error forms a double-sided distribution when using RSS mean, while it is approximately single-sided distributed using absolute RSS mean.

Figure 3: Absolute RSS mean has a smaller overall RSS error residual distribution.

observed RSS vectors in each state follow a multivariate Gaussian with shared covariance, as in [27], and denote

$$\delta_i(O) = P(O|S_i),$$

where

$$P(O|S_i) \sim \mathcal{N}(\mu_i, \Sigma).$$

However, the sensor model is imperfect because of the deep fading effect that can cause estimation error through only a few links[2]. Therefore, the cell associated with the maximum probability might be far from the ground truth.

Next, we look at the transition model. In each clock tick $t = 1, 2, ..., T$, the system makes a transition to state q_t. This process models the movement of a subject – the subject moves to a new cell in each tick. We choose a first order CRF, which means the next cell number depends on the current cell number, rather than any earlier history because we do not want to assume any specific human movement trajectories. In our model, subjects can either walk along a straight line, take turns or wander back and forth.

The subject's trajectory can thus be characterized as a parametric Markov random process with the *transition model* defined as the probability of a transition from state i at time $t-1$ to state j at time t in form of

$$T = P(q_t|q_{t-1}),$$

where

$$T_{ij} = P(q_t = S_j|q_{t-1} = S_i).$$

The intuition here is that people cannot walk through walls or cross rooms in a single tick. We believe these mobility constraints can be used to fix most of the errors in the sensor model caused by deep fades.

In our cell-based approach, we define the following:

Cell neighbors are a list of adjacent cells which can be entered from the current cell without violating mobility constraints.

Order of neighbor is defined as the number of cells a person must pass through to reach a specific cell from the current cell without violating mobility constraints. We assume the subject moves to a new cell every clock tick. For example, as far as cell i is concerned, the 1-order neighbors include its immediate adjacent cells, and its 2-order neighbors include the immediate adjacent cells of its 1-order neighbors (excluding i and i's first order neighbors).

---

[2]Because of deep fading from multipath, adjacent points can have dramatically different RSS values, leading to large estimation errors.

Trajectory ring with radius r is defined as the area consisting of cell i, i's 1-order neighbors, 2-order neighbors, ..., up to its r-order neighbors. Particularly, 0-order trajectory ring consists of all the cells.

Let $\Omega_r(i)$ be the cells included in i's r-trajectory ring and let $N_r(i)$ be the size of $\Omega_r(i)$. Our transition model thus becomes:

$$T_{ij} = \begin{cases} \frac{1}{N_r(i)} & \text{for} \quad j \in \Omega_r(i) \\ 0 & \text{for} \quad j \notin \Omega_r(i) \end{cases}$$

4.3 Localization Algorithm

Having constructed the sensor model and transition model, we can translate the problem of subject tracking to the problem of finding the most likely sequence of state transitions in a continuous time stream. The *Viterbi algorithm* [5] defines $V_j(t)$, the highest probability of a single path of length t which accounts for the first t observations and ends in state S_j:

$$V_j(t) = \underset{q_1, q_2, ..., q_{t-1}}{\text{argmax}} P(q_1 q_2 ... q_t = j, O_1 O_2 ... O_t | T, \delta).$$

By induction

$$V_j(1) = \delta_j(O_1),$$

$$V_j(t+1) = \underset{i}{\text{argmax}} V_i(t) T_{ij} \delta_j(O_{t+1}),$$

which is similar as discussed in [26].

Generalizing to the multi-subject case, we denote $\delta_{1:K}(O) = \{\delta_1(O), \delta_2(O), ..., \delta_K(O)\}$ from the sensor model to represent the likelihood of each state. We denote $Q = \{q^1, ..., q^C\}$, where C is the total number of present subjects. For the current state Q_t, we have $\binom{K}{C}$ possible permutations of subject locations. For each permutation j, we denote $Q_j = \{q^1, ..., q^C\}$ and compute the Viterbi score

$$F_j = \sum_{i=1}^{C} \delta_{q_t^i}(O_t) T_{q_{t-1}^i q_t^i}.$$

We then pick the j value that is associated with the maximum Viterbi score as the current state.

We describe our device-free multi-subject localization algorithm in Algorithm 3. We believe we can achieve best localization results when we consider 1 or 2-order trajectory ring, which is better than the 0-order case used in our earlier work [27], and is also confirmed by our experimental results presented in Section 6.

Algorithm 3: Trajectory-Based Device-free Multi-subject Localization Algorithm

---

input : $\mathcal{D}$- The training data collected from L links among K cells
T- The transition model
$O_{1:t}$- The testing data collected from L links when subjects are in unknown locations
C- The estimated number of present subjects in the deployed area
Q_1- The initial state(s) of the present subjects
output: $Q_{1:t}$- The most like sequence of the trajectories of the present subjects

---

1 **for** $i = 2 \rightarrow t$ **do**
2     $\delta_{1:K}(O_i) \leftarrow P(O_i|\mathcal{D})$
3     $\Pi \leftarrow$ is the set of all the possible permutations of $\binom{K}{C}$
4     $Q_i \leftarrow \mathrm{argmax}_{j \in \Pi} \texttt{ViterbiScore}(Q_{i-1}, Q_j, \delta_{1:K}(O_i), T)$

---

5. EXPERIMENTAL SETUP

In this section, we briefly describe the experimental setup, the data collection process and the metric we use for performance evaluation.

5.1 System Description

The radio devices used in our experiments contain a Chipcon CC1100 radio transceiver and a 16-bit Silicon Laboratories C8051-F321 microprocessor powered by a 20 mm diameter lithium coin cell battery, the CR2032. The receivers have a USB connector for loss-free data collection but are otherwise identical to the transmitters. In our experiments, the radio operates in the unlicensed bands at 909.1 MHz. Transmitters use MSK modulation, a 250 Kbps data rate, and a programmed output power of 0 dBm. Each transmitter periodically broadcasts a 10-byte packet (8 bytes of sync and preamble and 2 bytes of payload consisting of transmitter's id and sequence number) every 100 millisecond. When the receiver receives a packet, it measures the RSS values and wraps the transmitter id, receiver id, RSS, timestamp (on the receiver side) into a "data packet". The packets are forwarded to a centralized system where the data can be analyzed by independent "solvers" that perform various data processing functions. These include packet loss calculations [4], mobility detection [8], counting, localization, and data interpolation. More detail of the system can be found on the Owl Platform website [1].

5.2 Data Collection

In our experiments, the RSS data is collected as a mean value over a 1 second window for each link. We choose a 1 second window because a normal person can at most walk across one cell during a second. In the training phase, a single subject made random walk for 30 seconds in each cell and collected 30 RSS vectors as the profiling data. In this testing phase, we designed four scenarios for each environment, and in each scenario the subject(s) individually form a continuous mobility trajectory for about 30 seconds. The subjects are walking at a speed of about $0.5\ m$ per second. The training phase was performed in the early morning while the testing phase happened the afternoon of the same day.

5.3 Deployment Cost

In this study, we deployed our system in two different indoor settings which we will shown in Section 6. Our "solver" is running on a laptop (Intel i7-640LM 2.13GHz, 8GB RAM). For the 150 m^2 setting, it took 15 minutes to collect the training data, 0.003 seconds for the solver to fit the model parameters, and 3.4 seconds to compute the location-link correlation coefficients. The second

area was 2.7 times larger (400 m^2), but data collection only took 30 minutes, the solver was actually faster (0.002 seconds), and the time to compute the correlation coefficients only increased by a factor of about 1.5 (5.3 seconds).

5.4 Performance Metrics

We use the following performance metrics to measure our counting and localizing algorithms.

Counting Percentage is given by:

$$1 - \frac{|\hat{C} - C|}{C},$$

where $\hat{C}$ is the estimated subject count and C is the actual subject count.

Error Distance is defined as:

$$d(Q, \hat{Q}) = \frac{1}{C} \min_{\pi \in \Pi} \sum_{i=1}^{C} d(q^i, \hat{q}^{\pi(i)}),$$

where Π includes all the possible permutations of $\{1, 2, ..., C\}$, $d(q, \hat{q})$ is the Euclidean distance between the ground truth q and the estimated position $\hat{q}$. $Q = \{q^1, q^2, ..., q^C\}$ and $\hat{Q} = \{\hat{q}^1, \hat{q}^2, ..., \hat{q}^C\}$ are within the pre-profiled finite states $\mathcal{S} = \{S_1, S_2, ..., S_K\}$. In this study, q is the subject's actual location and $\hat{q}$ is her estimated location (i.e., center of the estimated cell).

6. EXPERIMENTAL RESULTS

In this section, we summarize the results we have obtained from two indoor settings. In each setting, we had multiple subjects each walking along a trajectory.

6.1 Results from Office Setting

Our first setting is a typical office environment, consisting of cubicles and aisles with a total area of 150 m^2. The environment is quite cluttered as shown in Figure 4(a). The area is broken down to 37 cells such as cubicles and aisle segments, as shown in Figure 4(b). We utilized 13 radio transmitters and 9 radio receivers, whose locations and corresponding link LoS's are shown in Figure 4(c). Here, we need to point out that these devices were installed for some earlier projects, not specifically for this one, and therefore, the link density per cell is non-uniform. This, however, represents a more realistic setting, through which we can show that SCPL can achieve good results without dedicated sensor deployment.

We had four subjects (A, B, C and D) in this series of experiments. We went through several example scenarios and illustrate them in Figure 5:

- *One Subject Scenario:* A left her boss's office, and walked along the aisle to her cubicle.

- *Two Subject Scenario:* When B entered the room, A was walking on the aisle towards him. B waited until they met and walked together for some time, and then separated to go back to their own seats.

- *Three Subject Scenario:* While A and B followed the movement patterns in the above two subject scenario, C walked on the other aisle from one cubicle to another.

- *Four Subject Scenario:* While A, B, and C followed the movement patterns in the above three subject scenario, D was sitting on her seat.

(a) Test Field
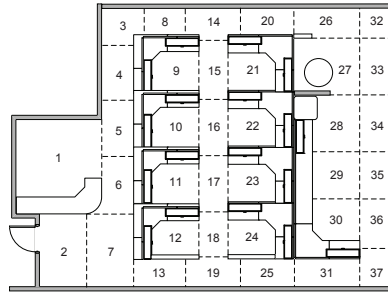
(b) Cell Locations
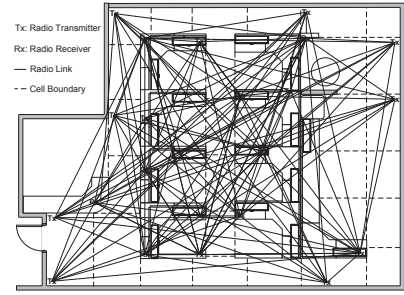
(c) Radio Link Distribution

Figure 4: In (a), we show the office in which we deployed our system. In (b), we show that the office deployment region is partitioned into 37 cubicle-sized cells of interest. In (c), we show the locations of the pre-installed 13 radio transmitters, 9 radio receivers and the corresponding Line-of-Sight links.
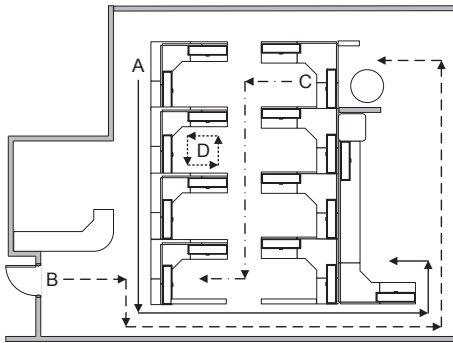

Figure 5: We show the experimental trajectories of subjects A, B, C and D in the office setting. Note the the trajectories of A and B are partially overlapped at the same time.
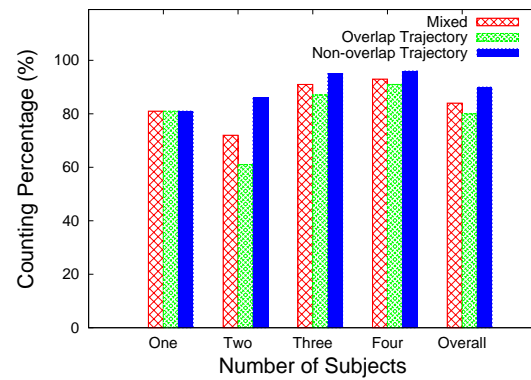
Figure 6: In a multi-subject case, our counting algorithm has a better performance when their trajectories are not overlapped than overlapped.
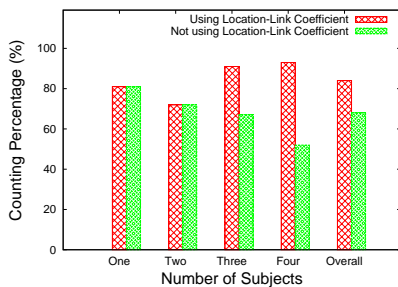

Figure 7: Counting percentage improvement when the RSS change is normalized by location-link coefficients in the office setting.
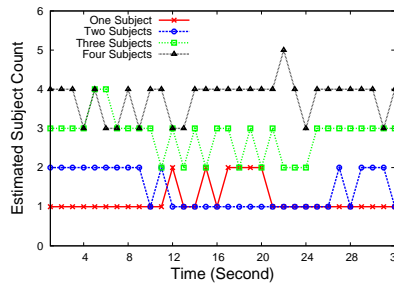

Figure 8: Estimated subject count over time using our successive cancellation-based counting algorithm in the office setting.
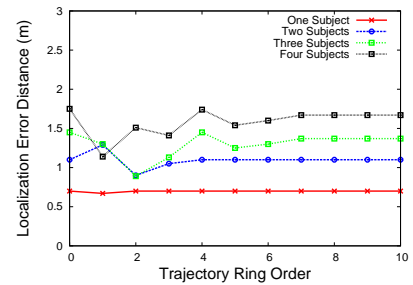

Figure 9: We achieve best localization accuracy averaging all the test cases when we adopt 1 or 2-order trajectory rings in the office setting.

6.1.1 Counting Results

The difficulty of subject counting increases when multiple subjects walk together (in the same cell). Thus, we present our counting results in the following three ways: (a) all the experimental data (referred to as *mixed*), (b) the experimental data for when multiple subjects walked together and thus had overlapping trajectories (referred to as *overlap trajectory*), and (c) the experimental data for

when multiple subject trajectories did not overlap (referred to as *non-overlap trajectory*). Figure 6 shows the counting percentages in all three cases.

We observe that when we have multiple subjects, the counting percentage is higher in the non-overlap trajectory case. The average counting percentage across all cases is 84%, the average counting percentage for non-overlap cases is 90%, and the average counting percentage for overlap cases is 80%.

Next, we show the performance improvement of subtracting a normalized RSS contribution by location-link coefficients compared to directly subtracting a cell's mean RSS change. We show the counting percentage results in these two cases in Figure 7. When we have one or two subjects, the non-linearity is not very obvious, and these two methods have very similar results. When we have more than two subjects, the non-linearity of the signal change becomes very pronounced, and using a normalized RSS contribution can yield better counting results. Specifically, we observe a 36% improvement with three subjects, and a 24% improvement with four subjects.

Finally, we show our subject counting results in Figure 8, in which all the four tests last 32 seconds. In the single-subject case, we see two individuals, between time tick 12 and 20. This is likely because there is an overestimate of γ near cells 13, 19, and 25, because of a denser than average link space or proximity to the receiver. In the two-subject case, we under-estimate the subject count by one between time tick 10 and 26 because the two subjects merged their trajectories in those time periods. The errors caused by temporally overlapping trajectories can also be easily addressed as follows. We continuously run the counting algorithm, and once we notice the estimated subject count suddenly drops, we check their locations before the sudden drop. If no subject's location was close to the exit, then we can conclude that two or more (depending upon the change in the count) were in close proximity. Of course, this information should be validated from the subject location information. For the three subjects case, we see the same problem when subjects A and B merge their trajectories. For the four subject case, this error is reduced a bit because subject D is always in cell 10, where has a relatively high density of radio links.

6.1.2 Localization Results

We show the mean of localization error distances in Figure 9 with different ring order parameters. In our setting, we choose 10 as the upper bound of the ring order because all cells are within 10 hops of each other.

Our first observation is that the use of the trajectory information can improve the localization performance by 13.6% – the overall mean localization error distance drops from $1.25m$ (with 0-order trajectory ring) [27] to about $1.08m$ (with 1-order trajectory ring). We note that the error distance for a single subject does not benefit from using trajectory information because the profiling data is good enough for this case [29, 27]. Multiple subjects, especially when they are close to each other, will cause non-linear radio interference, and thus the data collected from the mutually affected links alone cannot give very accurate localization results. Therefore, the sensor model alone is insufficient for high accuracies. Secondly, we observe that the localization results are less accurate in those cells with lower radio link densities, such as in cell 34-37, because subjects may cause negligible changes to the RSS space at a few points in those cells. Thirdly, trajectory information helps prevent the error distance increases dramatically as the increasing number of subjects. Finally, our environment is an office space consisting of cubicles and aisles, and the possible paths a subject can take are rather limited. As a result, we achieve the best localization accuracies with 1 or 2 order trajectory ring. Due to the movement constraints, a higher order trajectory ring has the same result as not considering any neighbors at all (i.e., 0 ring order). We hypothesize that this may not be true in a more open indoor environment such as (large) homes, malls and museums.

6.2 Results from Open Floor Space

The second test setting is a more open floor of total 400 m^2,

as shown in Figure 10(a). We used this setting to model an open hall with a few posters on exhibition, and SCPL can be used to detect traffic flow and infer the most popular poster. We deployed 12 transmitters and 8 receivers in such a way that the link density has a relatively even distribution across the cells, as shown in Figure 10(b). We would like to point out that we used fewer devices in this setting than in the previous one, though this one had a larger area. Also, this environment is even more challenging in that half of the radio devices are deployed on a wall which also has dozens of computers and other metal parts, significantly degrading radio propagation.

The space was partitioned into a uniform grid of 56 cells, and we involved four different subjects in this test and show their trajectories in Figure 10(c). We repeated the same four scenarios as in the previous setting. We plot our counting results in Figure 11. We achieve a 100% counting percentage when there was only a single subject, which is better than the previous setting because the link density is more even in this case. We achieve a counting percentage of 83%, 80%, and 82% for two, three and four subjects respectively, resulting in a 86% counting percentage in total. We have achieved better results when we normalize a subject's impact from a certain cell on the RSS with the location-link coefficients. We observe similar trends as in the previous setting: the results are the same for one or two subjects, and improved from 67% to 80%, and from 75% to 86% when we have three and four subjects, respectively. The estimated subject is shown in Figure 12.

We present the localization results in Figure 13. In the localization part, we observe similar patterns as in the previous setting: we achieve better localization accuracy using trajectory information. We achieve the best localization accuracy when we adopt the 2 order trajectory ring, which is 1.49 m, a 35% improved compared to the 0-order trajectory ring case [27].

7. LIMITATIONS AND FUTURE WORK

In this section, we discuss the limitation of SCPL.

7.1 Algorithms

Recognizing human mobility constraints in indoor environments leads to different trajectory-based tracking optimizations. Under our framework of discretized physical space, our localization algorithm relies on a greedy search for the optimal solution to find the most likely trajectories followed by the individuals. Unfortunately, this has factorial computation complexity because it involves C-permutations of K^3 and potentially introduces prohibitive overhead to meet real-time requirements, especially when K grows rapidly in a large-scale environment. However, as we observed from the experimental results from the two different settings, we have achieved the best localization accuracies using only the 1 or 2-order trajectory ring, which means we can not only achieve good accuracy, but also significantly reduce the computational complexity by reducing the permutation space from $\binom{K}{C}$ to $\binom{K'}{C}$, where K' is the cell union of each individual's 1 or 2-order trajectory rings. Under 1-order trajectory ring, it took 0.87 seconds and 0.88 seconds to count and localize four subjects in our two different settings respectively. We would expect that it will take more than 1 second to track at least five subjects, which fails to afford real-time tracking requirement with this hardware. Another family of trajectory based tracking incorporates a particle filter [18], such as the one used in [24, 13]. However, the primary weakness of particle filters is the computational complexity required to run the algorithm for the large number of particles needed to achieve accurate re-
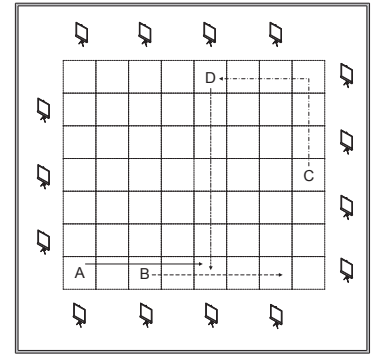
---

[3]C is the subject count and K is the total number of cells.
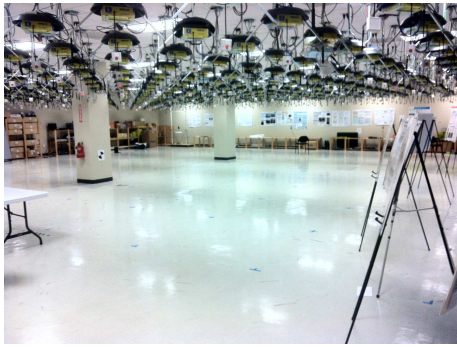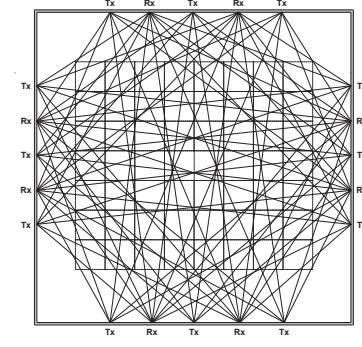
| (a) Test Field | (b) Radio Link Distribution | (c) Test Trajectories |

Figure 10: In (a), we show the open floor space used for poster exhibition in which we deployed our system. In (b), we show the locations of the 12 radio transmitters, 8 radio receivers and the corresponding Line-of-Sight links. In (c), we show the experimental trajectories of subjects A, B, C and D in the open floor space which is partitioned into a uniform grid of 56 cells.
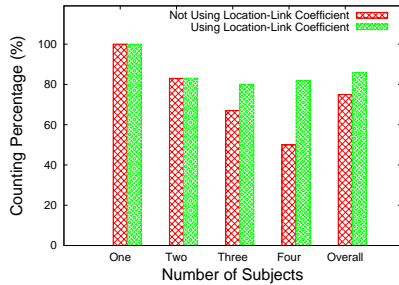

Figure 11: Counting percentage improvement when the RSS change is normalized by location-link coefficients in the open floor space.
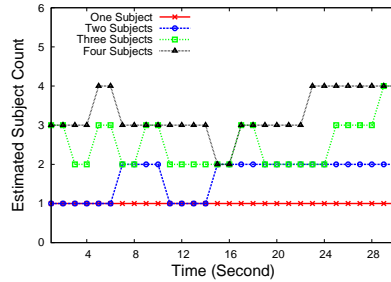

Figure 12: Estimated subject count over time using our successive cancellation-based counting algorithm in the open floor space.
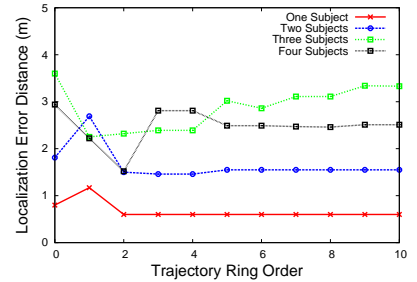

Figure 13: We consistently achieve best localization accuracy when we adopt 1 or 2-order trajectory rings in the open floor space

sults. For example, 500 particles were needed for tracking each individual and it took 7.6 seconds for four subjects in each time step, as reported in [13]. Overall, there is plenty space to optimize the trade-off between accuracy and computational cost in tracking multiple subjects for future work.

7.2 Long-term Test

In a long-run test, any RF-based localization schemes suffer not only from temporal fading, but also from environmental changes. A small piece of metal can change the tuning of the antenna shift the radiation pattern or even the radio frequency of the nearby transmitter or receiver. Either or both of these effects can change the underlying propagation pattern and, hence, the RSS values on the links. To avoid frequent manual recalibration, we present two schemes in our earlier work [27, 28] to maintain the localization accuracy over a long-term test. In [27], we simply remove the radio links experiencing deep fading by watching RSS values over time, which is able to maintain a cell estimation accuracy of 90% over one month. In [28], we present a camera-assisted auto recalibration – when the camera occasionally turns on, it localizes the subject and calibrates the RF data automatically. Both schemes have limitations: the performance of the first scheme will degrade when the number of remaining links is too small, while the second one needs extra hardware. Realizing these limitations, we will investigate sophisticated auto-calibration methods as part of the future work.

8. RELATED WORK

In this section, we briefly review the related literature in RF-based counting and localizing device-free human subjects.

8.1 Device-Free Counting

Nakatsuka et al. [12] first demonstrated the feasibility of using radio signal strength to estimate the crowd density. The authors setup two radio nodes and observe that RSS decreases as the number of subjects increases when they are all sitting between the nodes. We, however, point out that SCPL is the first work that systematically counts device-free subjects in large scale deployment, to our best knowledge.

8.2 Device-Free Localization

In 2006, Woyach et al. [25] first experimentally demonstrated the feasibility of localizing device-free subjects by observing a difference in RSS changes by a subject moving between (resulting signal shadowing effect) and in the vicinity (causing small-scale fading) of a pair of transmitter and receiver. From then on, several DfP approaches have been proposed in the literature, which can be broadly categorized into two groups as follows.

Location-based schemes: This approach is also known as "fingerprinting", a popular approach for RF-based localization. It was first studied in [29] in the context of passive localization. The authors first collect a radio map with the subject present in a few prede-

	Grid Array [30]	RTI [7]	NUZZER [19]	SCPL
Meausred physical quantity	RSS variance	RSS attenuation	RSS change	RSS change
Non-LoS localization	No	Yes	Yes	Yes
Nodes density	High	High	Low	Median
Prior knowledge of node locations	Yes	Yes	No	No
Tracking static subjects	No	Yes	Yes	Yes
Deployment scale	Median	Small	Large	Large
Training overhead	Low	Low	High	Median

Table 1: Comparison of different RF-based passive localization systems.

termined locations, and then map the test location to one of these trained locations based upon observed radio signals. This method explicitly measures the multipath effect on RSS in each different position, and thus avoids modeling errors. In addition, it does not require a node deployment as dense as in link-based schemes because when the subject is in the position has no intersection with any radio LoS links, the RSS ground truth still can provide a distinguishable record from other positions. This work is extended to a much larger deployment in Nuzzer [19]. In [27], Xu et al. propose to formulate this localization problem into a probabilistic classification problem and use a cell-based calibration with random walk method profiling the system in order to mitigate the error caused by the multipath effect in cluttered indoor environments, improve the localization accuracy and meanwhile reduce the profiling overhead. However, the downside of fingerprinting is also evident: the calibration procedure is relatively tedious.

Link-based schemes: These techniques look for those radio links close to the target subjects and further determine the locations of the targets based on the RSS dynamics. Zhang et al. [31] set up a sensor grid array on the ceiling to track subjects on the ground. An "influential" link is one whose RSS variance exceeds a empirical threshold. The authors determine a subject's location based upon the observation that these influential links tend to cluster around the subject. This technique forms a consistent link-based model to relate the subject's location relative to the radio link locations. In [32]. the authors extend their algorithms to track up to subjects separated by at least 5 m. In [30], the monitored area is partitioned into different triangle sections, and the nodes in neighbor section are working at different communication channels to reduce the interference among nodes. The authors applied support vector regression model to track up to two subjects. The fundamental limitations of this series of work is that (i) not all the monitored places have the facilities to mount nodes on the ceiling; (ii) this work uses RSS variance as the data primitive, which is essentially the amplitude and phase shift of the ground reflection multipath caused by the of human subjects only in motion. In other words, the system might fail to work if the subjects stop walking. Another sets of work following Link-based DfP is radio tomographic imaging (RTI). Wilson et al. [22] use tomographic reconstruction to estimate an image of human presence in the deployment area of the network. RSS attenuation is used as data primitive in [22], which effectively works in outdoor or uncluttered indoor space without rich multipath. Recognizing the nature of multipath fading, Wilson et al. defined the concept of fade-level [24], which captures the ambient RSS characteristics of each link and categorize the links into deep fade (the RSS will increase on average when the LoS is blocked) and antifade (the RSS decreases when the LoS is obstructed) through fitting the calibration data to a skewed Laplace distribution. The authors demonstrate this technique's effectiveness through testing in same setting over time and a totally different setting without the effort of

re-estimating the model parameters. Kaltiokallio et al. [7] further exploit channel diversities to enhance the tracking accuracy. Taking the framework of RTI, another sets of work is done based on sequential Monte Carlo sampling techniques. Chen et al. [2] propose to use auxiliary particle filtering method to simultaneously localize the nodes and a single subject in an outdoor setting. In [20], the author introduce a measurement model which assumes the attenuation in RSS due to the simultaneous presence of multiple subjects on the LoS is approximately equal to the sum of the attenuations caused by the individuals. This model is then applied in [13, 14] for tracking up to four subjects in outdoor and indoor settings. In general, link-based schemes have two advantages: (i) the algorithms are robust to the environmental change because the subject's location is directly estimated based on its relative distance to each individual radio link LoS; (ii) it requires less calibration effort - only sensor locations and ambient RSS for each link is needed. However, it requires a dense nodes deployment to provide enough radio LoS links to cover all the physical space.

Finally, we summarize the differences between our system and the recent DfP RF-based localization systems in Table 1.

9. CONCLUSION

In this paper, we present SCPL, an accurate counting and localization system for device-free subjects. We demonstrate the feasibility of using the profiling data collected with only a single subject present to count and localize multiple subjects in the same environment with no extra hardware or data collection. Through extensive experimental results, we show that SCPL works well in two different typical indoor environments of 150 m^2 (office cubicles) and 400 m^2 (open floor plan) deployed using an infrastructure of only 20 to 22 devices. In both spaces, we can achieve about an 86% average counting percentage and 1.3 m average localization error distance for up to 4 subjects. Finally, we shows that though a complex environment like the office cubicles is expected to have worse radio propagation, we can leverage the increased mobility constraints that go with a complex environment to maintain or even improve accuracy in these situations.

Finally, we point out that if we rely on a single subject's training data, the number of subjects that can be accurately counted and localized is rather limited. We had success with up to 4 subjects, but were not very successful with more subjects. In our future work, we will look at how we can accurately localize a larger number of subjects with reasonable overheads.

Acknowledgments

10. REFERENCES

[1] Owl platform: The great owl watches all things. http://www.owlplatform.com/.

[2] X. Chen, A. Edelstein, Y. Li, M. Coates, M. Rabbat, and A. Men. Sequential monte carlo for simultaneous passive device-free tracking and sensor localization using received signal strength measurements. In *ACM/IEEE IPSN*, 2011.

[3] D. De, W.-Z. Song, M. Xu, C.-L. Wang, D. Cook, and X. Huo. Findinghumo: Real-time tracking of motion trajectories from anonymous binary sensing in smart environments. In *IEEE ICDCS*, 2012.

[4] B. Firner, C. Xu, R. Howard, and Y. Zhang. Multiple receiver strategies for minimizing packet loss in dense sensor networks. In *ACM MobiHoc*, 2010.

[5] G. D. Forney Jr. The viterbi algorithm. *Proceedings of the IEEE*, 61(3), 1973.

[6] T. W. Hnat, E. Griffiths, R. Dawson, and K. Whitehouse. Doorjamb: unobtrusive room-level tracking of people in homes using doorway sensors. In *ACM SenSys*, 2012.

[7] O. Kaltiokallio, M. Bocca, and N. Patwari. Enhancing the accuracy of radio tomographic imaging using channel diversity. In *IEEE MASS*, 2012.

[8] K. Kleisouris, B. Firner, R. Howard, Y. Zhang, and R. P. Martin. Detecting intra-room mobility with signal strength descriptors. In *ACM MobiHoc*, 2010.

[9] J. Krumm, S. Harris, B. Meyers, B. Brumitt, M. Hale, and S. Shafer. Multi-camera multi-person tracking for easyliving. In *IEEE VS*, 2000.

[10] J. D. Lafferty, A. McCallum, and F. C. N. Pereira. Conditional random fields: Probabilistic models for segmenting and labeling sequence data. In *ICML*, 2001.

[11] R. S. Moore, R. Howard, P. Kuksa, and R. P. Martin. A geometric approach to device-free motion localization using signal strength. Technical report, Technical Report, Rutgers University, 2010.

[12] M. Nakatsuka, H. Iwatani, and J. Katto. A study on passive crowd density estimation using wireless sensors. In *ICMU*, 2008.

[13] S. Nannuru, Y. Li, M. Coates, and B. Yang. Multi-target device-free tracking using radio frequency tomography. In *IEEE ISSNIP*, 2011.

[14] S. Nannuru, Y. Li, Y. Zeng, M. Coates, and B. Yang. Radio frequency tomography for passive indoor multi-target tracking. *IEEE Transactions on Mobile Computing*, PP(99), 2012.

[15] R. J. Orr and G. D. Abowd. The smart floor: a mechanism for natural user identification and tracking. In *ACM CHI*, 2000.

[16] N. Patwari and J. Wilson. Rf sensor networks for device-free localization: Measurements, models, and algorithms. *Proceedings of the IEEE*, 98(11), 2010.

[17] T. Rappaport. *Wireless Communications: Principles and Practice*. Prentice Hall PTR New Jersey, 2nd edition, 2001.

[18] B. Ristic, S. Arulampalm, and N. Gordon. *Beyond the Kalman filter: Particle filters for tracking applications*. Artech House Publishers, 2004.

[19] M. Seifeldin and M. Youssef. A deterministic large-scale device-free passive localization system for wireless environments. In *ACM PETRA*, 2010.

[20] F. Thouin, S. Nannuru, and M. Coates. Multi-target tracking for measurement models with additive contributions. In *IEEE FUSION*, 2011.

[21] M. Valtonen, J. Maentausta, and J. Vanhala. Tiletrack: Capacitive human tracking using floor tiles. In *IEEE PerCom*, 2009.

[22] J. Wilson and N. Patwari. Radio tomographic imaging with wireless networks. *IEEE Transactions on Mobile Computing*, 9(5), 2010.

[23] J. Wilson and N. Patwari. See-through walls: Motion tracking using variance-based radio tomography networks. *IEEE Transactions on Mobile Computing*, 10(5), 2011.

[24] J. Wilson and N. Patwari. A fade level skew-laplace signal strength model for device-free localization with wireless networks. *IEEE Transactions on Mobile Computing*, 11(6), 2012.

[25] K. Woyach, D. Puccinelli, and M. Haenggi. Sensorless sensing in wireless networks: Implementation and measurements. In *IEEE WiOpt*, 2006.

[26] C. Xu, B. Firner, Y. Zhang, R. Howard, and J. Li. Trajectory-based indoor device-free passive tracking. In *IWMS*, 2012.

[27] C. Xu, B. Firner, Y. Zhang, R. Howard, J. Li, and X. Lin. Improving rf-based device-free passive localization in cluttered indoor environments through probabilistic classification methods. In *ACM/IEEE IPSN*, 2012.

[28] C. Xu, M. Gao, B. Firner, Y. Zhang, R. Howard, and J. Li. Towards robust device-free passive localization through automatic camera-assisted recalibration. In *ACM SenSys*, 2012.

[29] M. Youssef, M. Mah, and A. Agrawala. Challenges: device-free passive localization for wireless environments. In *ACM MobiCom*, 2007.

[30] D. Zhang, Y. Liu, and L. Ni. Rass: A real-time, accurate and scalable system for tracking transceiver-free objects. In *IEEE PerCom*, 2011.

[31] D. Zhang, J. Ma, Q. Chen, and L. M. Ni. An rf-based system for tracking transceiver-free objects. In *IEEE PerCom*, 2007.

[32] D. Zhang and L. M. Ni. Dynamic clustering for tracking multiple transceiver-free objects. In *IEEE PerCom*, 2009.